JUSTC

Article

http://justc.ustc.edu.cn

Received: November 22, 2023; Accepted: March 05, 2024

On capped Higgs positivity cone

Dong-Yu Hong[1], Zhuo-Hui Wang[1], and Shuang-Yong Zhou[1,2] ✉

[1]*Interdisciplinary Center for Theoretical Study, University of Science and Technology of China, Hefei 230026, China;*
[2]*Peng Huanwu Center for Fundamental Theory, Hefei 230026, China*

✉Correspondence: Shuang-Yong Zhou, E-mail: zhoushy@ustc.edu.cn

Graphical abstract

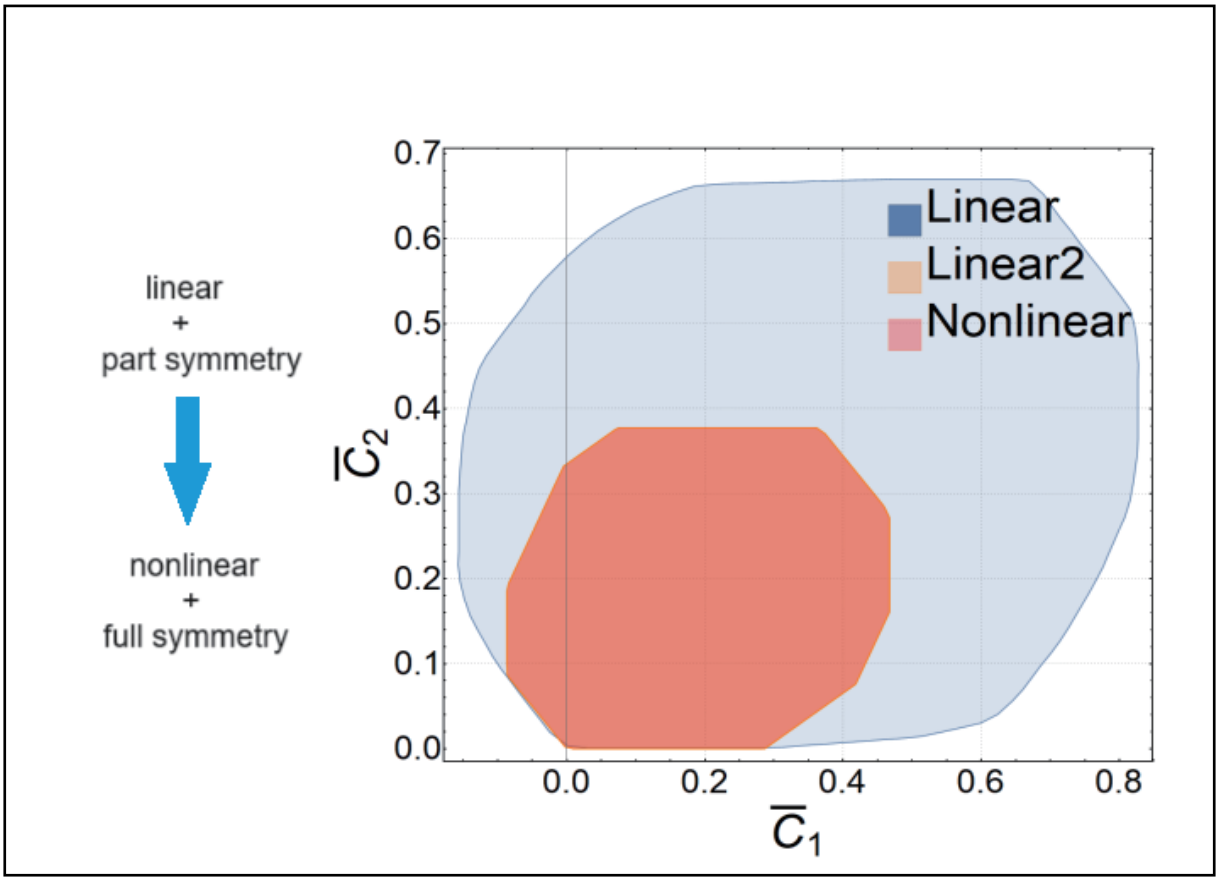

The bound on two dim-8 coefficients of the Higgs. The orange and red regions represent the results of the current paper using linear and nonlinear unitarity conditions, respectively, with all the symmetries of the SMEFT Higgs included, while the blue region represents the previous result using linear unitarity conditions but without full Higgs symmetry.

Public summary

- We cap the positivity cone from above by making fuller use of unitarity conditions.
- We present a systematic method for obtaining more robust positivity bounds by employing nonlinear unitarity conditions and incorporating all symmetries of the SMEFT Higgs.
- We explain the differences in performance between linear and nonlinear unitarity conditions, demonstrating how the nonlinear unitarity conditions can be reduced to the linear ones.

Citation: Hong D Y, Wang Z H, Zhou S Y. On capped Higgs positivity cone. *JUSTC*, **2024**, 54(7): 0705. DOI: 10.52396/JUSTC-2023-0159

JUSTC

Article

http://justc.ustc.edu.cn

Received: November 22, 2023; Accepted: March 05, 2024

On capped Higgs positivity cone

Dong-Yu Hong[1], Zhuo-Hui Wang[1], and Shuang-Yong Zhou[1,2] ✉

[1]*Interdisciplinary Center for Theoretical Study, University of Science and Technology of China, Hefei 230026, China;*
[2]*Peng Huanwu Center for Fundamental Theory, Hefei 230026, China*

✉Correspondence: Shuang-Yong Zhou, E-mail: zhoushy@ustc.edu.cn

Cite This: *JUSTC*, **2024**, 54(7): 0705 (11pp)

Read Online

Abstract: The Wilson coefficients of the standard model effective field theory are subject to a series of positivity bounds. It has been shown that while the positivity part of the Ultraviolet (UV) partial wave unitarity leads to the Wilson coefficients living in a convex cone, further including the nonpositivity part caps the cone from above. For Higgs scattering, a capped positivity cone was obtained using a simplified, linear unitarity condition without utilizing the full internal symmetries of Higgs scattering. Here, we further implement stronger nonlinear unitarity conditions from the UV, which generically gives rise to better bounds. We show that, for the Higgs case in particular, while the nonlinear unitarity conditions per se do not enhance the bounds, the fuller use of the internal symmetries do shrink the capped positivity cone significantly.

Keywords: positivity bounds; standard model effective field theory (SMEFT); Higgs

CLC number: O572.2 **Document code:** A

1 Introduction

Effective field theories (EFTs) serve as valuable tools for describing low-energy physics without explicit knowledge of the intricate high energy theory. The effectiveness of an EFT depends heavily on precisely determining its Wilson coefficients, which often poses a significant challenge because there can be numerous of them or they might be rather difficult to measure. Recent developments highlight that the general parameter space for the Wilson coefficients is mostly inconsistent with the fundamental principles of S-matrix theory, such as causality/analyticity and unitarity, except for a small subspace defined by the positivity bounds (see, for example, Refs. [1–43] and Ref. [44] for a review).

The positivity bounds have been used to constrain the standard model effective field theory (SMEFT)[10, 11, 45–69]. The SMEFT parameterizes generic new physics beyond the standard model (SM) based on the SM field content and symmetries, and has been gaining popularity in both theoretical and experimental communities in the absence of new particle discoveries at the Large Hadron Collider (LHC). The SMEFT contains numerous Wilson coefficients particularly from dimension-8[70, 71] and beyond, as the SM is a theory with many field degrees of freedom.

For a theory with multiple degrees of freedom, the positivity bounds significantly reduce the extensive parameter space. For instance, in vector boson scattering (VBS), the elastic positivity bounds can confine the physical dimension-8 Wilson coefficient space to approximately 2% of the total space[45, 46, 72]. For the 10D dimension-8 VBS subspace involving only the transverse vector bosons, generalized elastic positivity bounds reduce the viable parameter space to about 0.7% of the total[49]. Futhermore, for the s^2 amplitude coefficients (s,t,u being the standard Mandelstam variables), the optimal positivity bounds can be obtained by a convex geometry approach[10, 12, 49, 59]. When there are sufficient symmetries in the sub-sector we are interested in, one can use a group-theoretical method to compute the positivity cone, and the extremal rays of the cone in this case can be very useful in reverse engineering the UV theory in the event of an observation of non-zero Wilson coefficients[10, 12, 59]. Generically, with fewer symmetries, one can employ a semi-definite programming (SDP) method to compute the the s^2 positivity cone[11].

The preceding s^2 positivity cones are obtained by using only the positivity part of the UV unitarity conditions. Ref. [73] has initiated the use of the non-positivity parts of the UV unitarity conditions to constrain the SMEFT coefficients, focusing on the scattering involving only the complex Higgs modes. Building upon the methods introduced in Refs. [6, 7, 27], the numerical bounds of Ref. [73] are obtained by discretizing the UV scales in the fixed-t dispersion relations and using the null constraints and linear programming to extract the constraints on the Wilson coefficients. Specifically, Ref. [73] derived a set of linear conditions from (nonlinear) partial wave unitarity, which allows the numerical optimizaiton to be easily carried out with some simple `Mathematica` coding.

In this paper, we will revisit the capped positivity bounds on the SMEFT Higgs sector, making use of the nonlinear unitarity conditions on the imaginary part of the UV amplitudes. We will also more carefully take into account all available symmetries of the SMEFT Higgs Lagrangian. With these improvements, significantly better upper bounds are obtained. The paper is organized as follows. In Section 2, we will first derive the scattering amplitudes and dispersion rela-

DOI: 10.52396/JUSTC-2023-0159
JUSTC, **2024**, 54(7): 0705

tions from the SMEFT Lagrangian pertaining to the Higgs, and then introduce the null constraints and the nonlinear UV unitarity conditions we will use in this paper. In Section 3, we briefly set up the numerical optimization scheme for computing the two-sided, optimal numerical bounds. In Section 4, we present our results on the capped Higgs positivity cone, and compare with those obtained in Ref. [73]. We will see that, carefully taking into account the SMEFT Higgs symmetries, the linear unitarity bounds actually give rise to the same positivity bounds as those from the nonlinear unitarity conditions. We conclude in Section 5. In Appendix A.1, we will show that the linear unitarity conditions of Ref. [73] can be derived from the nonlinear unitarity conditions. In Appendix A.2, we will use a bi-scalar theory as an example to demonstrate that generically the nonlinear unitarity conditions are stronger than the linear ones.

2 Model and setup

In this section, we derive the amplitudes for Higgs scattering in the SMEFT and the corresponding fixed-t dispersion relations that are used to extract positivity bounds on the dim-8 Wilson coefficients. Then, we proceed to obtain the so-called null constraints by imposing st crossing symmetries on these dispersion relations, and present the nonlinear unitarity conditions we will use in this paper. Combining these ingredients together, we will derive two-sided bounds for the dim-8 Higgs coefficients in the following sections.

2.1 Amplitudes and dispersion relations

In the SMEFT, the Higgs retains the same symmetry as in the SM and is a SU(2) doublet. We shall parameterize the Higgs doublet with two complex fields

$$H=\frac{1}{\sqrt{2}}\begin{pmatrix}\phi_1\\ \phi_2\end{pmatrix}, \tag{1}$$

and will use $\bar{\mathrm{i}}$ to denote the antiparticle of particle i. Thanks to the SU(2) internal symmetry, a generic 2-to-2 Higgs scattering amplitude can be parameterized by the invariant tensors of the SU(2) symmetry $\mathcal{M}^{\mathrm{ij\bar{k}\bar{l}}}(s,t)=\delta_{\mathrm{ij}}\delta_{\mathrm{\bar{k}\bar{l}}}\alpha(s,t)+\delta_{\mathrm{i\bar{l}}}\delta_{\mathrm{j\bar{k}}}\beta(s,t)$. Here we choose all the particles to be all-ingoing for the amplitudes. The rest amplitudes are related to $\mathcal{M}^{\mathrm{ij\bar{k}\bar{l}}}$ by crossing. The su crossing symmetry implies that $\mathcal{M}^{\mathrm{ij\bar{k}\bar{l}}}(s,t)=\mathcal{M}^{\mathrm{i\bar{l}\bar{k}j}}(u,t)$, which means that we must have $\alpha(u,t)=\beta(s,t)$. Thus, we can express the Higgs amplitude as

$$\mathcal{M}^{\mathrm{ij\bar{k}\bar{l}}}(s,t)=\delta_{\mathrm{ij}}\delta_{\mathrm{\bar{k}\bar{l}}}f(s,t)+\delta_{\mathrm{i\bar{l}}}\delta_{\mathrm{j\bar{k}}}f(u,t). \tag{2}$$

Suppose that below the EFT cutoff the theory is weakly coupled so that we can take the tree level approximation. Then, at low energies, we can parameterized $f(s,t)$ as

$$f_{\mathrm{EFT}}(s,t)=a_1s+a_2t+b_1s^2+b_2st+b_3t^2+c_1s^3+c_2s^2t+\cdots, \tag{3}$$

which is the tree level approximation of $f(s,t)$ in the EFT region. We will be interested in constraining the Wilson coefficients of the dimension-8 SMEFT operators that will contribute to the 2-to-2 Higgs scattering. There are three of these operators, all of which contain four derivatives and are parameterized as follows

$$\begin{aligned}\mathcal{L}_{\mathrm{SMEFT}}\supset\ & C_1(D_\mu H^\dagger D_\nu H)(D^\nu H^\dagger D^\mu H)+C_2(D_\mu H^\dagger D_\nu H)\\ & (D^\mu H^\dagger D^\nu H)+C_3(D^\mu H^\dagger D_\mu H)(D^\nu H^\dagger D^\nu H),\end{aligned} \tag{4}$$

where D^μ is the gauge covariant derivatives. Matching the C_i coefficients with the amplitude coefficients in $f_{\mathrm{EFT}}(s,t)$, we find that

$$C_1=b_3,\quad C_2=2b_2-b_3,\quad C_3=2b_1-b_3. \tag{5}$$

To make use of the null constraints and partial wave unitarity, we need to derive the dispersion relations where the UV amplitudes are expanded with partial waves. To that end, we shall perform the following partial wave expansion

$$\mathcal{M}^{1\bar{1}2\bar{2}}(s,t)=16\pi\sum_\ell(2\ell+1)P_\ell(1+\frac{2t}{s})a_\ell^s(s), \tag{6}$$

$$\mathcal{M}^{12\bar{1}\bar{2}}(s,t)=16\pi\sum_\ell(2\ell+1)P_\ell(1+\frac{2t}{s})a_\ell^t(s), \tag{7}$$

$$\mathcal{M}^{1\bar{2}2\bar{1}}(s,t)=16\pi\sum_\ell(2\ell+1)P_\ell(1+\frac{2t}{s})a_\ell^u(s), \tag{8}$$

where $P_\ell(x)$ is the Legendre polynomial and we have defined

$$a_\ell^s(s)=a_\ell^{1\bar{1}2\bar{2}}(s),\quad a_\ell^t(s)=a_\ell^{12\bar{1}\bar{2}}(s),\quad a_\ell^u(s)=a_\ell^{12\bar{2}\bar{1}}(s). \tag{9}$$

Note that a_ℓ^s, a_ℓ^t, and a_ℓ^u are related, as they are all expanded from the same function but with different arguments:

$$\mathcal{M}^{1\bar{1}2\bar{2}}(s,t)=f(s,t),\ \mathcal{M}^{12\bar{1}\bar{2}}(s,t)=f(t,s),\ \mathcal{M}^{12\bar{2}\bar{1}}(s,t)=f(u,t). \tag{10}$$

These relations will be taken into account by supplying the dispersion relations with null constraints. The expansions for the other amplitudes can be related to the above three via $a_\ell^{ijkl}(s)=(-1)^\ell a_\ell^{ijlk}(s)$. (We adopt the convention that the indices i, j, k, l refer to particles, indices $\bar{\mathrm{i}},\bar{\mathrm{j}},\bar{\mathrm{k}},\bar{\mathrm{l}}$ refer to antiparticles, and indices i,j,k,l refer to particles or antiparticles.) More explicitly, we have

$$\begin{aligned}\mathcal{M}^{1\bar{1}2\bar{2}}(s,u)&=\mathcal{M}^{1\bar{1}2\bar{2}}(s,t)=16\pi\sum_\ell(2\ell+1)P_\ell(1+\frac{2t}{s})a_\ell^{1\bar{1}2\bar{2}}(s)\\ &=16\pi\sum_\ell(2\ell+1)P_\ell(1+\frac{2t}{s})(-1)^\ell a_\ell^s(s),\end{aligned} \tag{11}$$

$$\begin{aligned}\mathcal{M}^{1\bar{1}2\bar{2}}(u,s)&=\mathcal{M}^{1\bar{1}2\bar{2}}(u,t)=\mathcal{M}^{12\bar{2}\bar{1}}(s,t)\\ &=16\pi\sum_\ell(2\ell+1)P_\ell(1+\frac{2t}{s})a_\ell^{12\bar{2}\bar{1}}(s)\\ &=16\pi\sum_\ell(2\ell+1)P_\ell(1+\frac{2t}{s})(-1)^\ell a_\ell^t(s),\end{aligned} \tag{12}$$

$$\begin{aligned}\mathcal{M}^{1\bar{1}2\bar{2}}(t,u)&=\mathcal{M}^{12\bar{1}\bar{2}}(u,t)=\mathcal{M}^{12\bar{1}\bar{2}}(s,t)\\ &=16\pi\sum_\ell(2\ell+1)P_\ell(1+\frac{2t}{s})a_\ell^{12\bar{1}\bar{2}}(s)\\ &=16\pi\sum_\ell(2\ell+1)P_\ell(1+\frac{2t}{s})(-1)^\ell a_\ell^u(s).\end{aligned} \tag{13}$$

DOI: 10.52396/JUSTC-2023-0159
JUSTC, 2024, 54(7): 0705

With the above ingredients as well as the Froissart–Martin bound[74, 75], a relative simple use of the residue theorem on the complex s plane for fixed t, plus some straightforward algebra, allows us to derive the twice subtracted dispersion relations for the amplitudes (for example, Ref. [2]):

$$\sum_{\text{EFT poles}} \frac{\mathcal{M}^{ijkl}(\mu,t)}{\mu-s} = z_0(t)+z_1(t)s+ \left\langle \frac{s^2P_\ell(1+2t/\mu)}{\mu^2(\mu-s)}\rho_\ell^{ijkl}(\mu)+\frac{u^2P_\ell(1+2t/\mu)}{\mu^2(\mu-u)}\rho_\ell^{ilkj}(\mu)\right\rangle, \tag{14}$$

where we have defined

$$<\cdots>=16\sum_\ell\int_{\Lambda^2}^\infty \mathrm{d}\mu(2\ell+1)\cdots \tag{15}$$

and "EFT poles" denotes the poles of the amplitudes $\mathcal{M}^{ijkl}$ in the low energy EFT region, Λ is the EFT cutoff and $\rho_\ell^{ijkl}(\mu)=\mathrm{Im}a_\ell^{ijkl}(\mu)$. $z_n(t)$ are some functions of t that we will not use in this paper, as we are constraining the coefficients in front of the terms s^nt^m with $n\geq 2$. The fact that a fixed t dispersion relation naturally constrains the terms s^nt^m with $n\geq 2$ is related to the Froissart-Martin bound. Specifically, the Froissart–Martin bound states that $\lim_{s\to\infty}\mathcal{M}/s^2=0$ for fixed t. Therefore, a direct application of Cauchy's integral formula on $\mathcal{M}$ leads to a dispersion relation with various diverging terms, which should cancel among themselves. The solution is to apply a twice subtraction, which directly allows us to constrain terms with s^nt^m, $n\geq 2$. In other words, on the right hand side of the dispersion relation, we have the $z_0(t)$ and $z_1(t)s$ term, where $z_0(t)$ and $z_1(t)$ contain some unknown information related to various contour integrals going like $\int \mathrm{d}\mu\mathrm{Im}\mathcal{M}/(\mu-s)$. Thus, the s^0 and s^1 EFT term on the left hand side can not be constrained. (Of course, with crossing symmetries, coefficients in $z_n(t)$ can often be related to the $s^{n>2}t^m$ coefficients and thus also be bounded.) Now, Eq. (14) is convergent on both sides of the equality, so we can taylor-expand both sides and match the coefficients in front of s^nt^m, which gives a set of sum rules that will be used to derive the positivity bounds. For example, let us consider the dispersion relation of amplitude $\mathcal{M}^{1\bar{1}2\bar{2}}(s,t)$. Taylor-expanding both sides of the dispersion relation, we get

$$\begin{aligned} &a_1s+a_2t++b_1s^2+b_2st+b_3t^2+c_1s^3+c_2s^2t+\cdots=z_0(t)+\\ &\left\langle\frac{\rho_\ell^s(\mu)+\rho_\ell^u(\mu)}{\mu^3}\right\rangle t^2+\left(z_1(t)+2\left\langle\frac{\rho_\ell^u(\mu)}{\mu^3}\right\rangle t\right)s+\\ &\left\langle\frac{(\rho_\ell^s(\mu)+\rho_\ell^u(\mu))}{\mu^3}\right\rangle s^2+\left\langle\frac{\rho_\ell^s(\mu)-\rho_\ell^u(\mu)}{\mu^4}\right\rangle s^3+\\ &\left\langle\frac{(\ell(1+\ell)\rho_\ell^s(\mu)+(-3+\ell+\ell^2)\rho_\ell^u(\mu)}{\mu^4}\right\rangle s^2t+\cdots \end{aligned} \tag{16}$$

and matching the coefficients in front of the terms s^nt^m, we can get

$$b_1=\left\langle\frac{\rho_\ell^s(\mu)+\rho_\ell^u(\mu)}{\mu^3}\right\rangle, \tag{17}$$

$$c_1=\left\langle\frac{\rho_\ell^s(\mu)-\rho_\ell^u(\mu)}{\mu^4}\right\rangle, \tag{18}$$

$$c_2=\left\langle\frac{(\ell(1+\ell)\rho_\ell^s(\mu)+(-3+\ell+\ell^2)\rho_\ell^u(\mu)}{\mu^4}\right\rangle, \tag{19}$$

$$\vdots$$

These sum rules connect the unknown UV amplitudes with the low energy Wilson coefficients. The positivity bounds are the imprints of the UV information on the IR physics, passed down by these dispersion relations/sum rules.

2.2 Null constraints

The fixed t dispersion relations above or the sum rules extracted from them only include part of the full crossing symmetries of the amplitudes. To utilize the full crossing symmetries, we can simply impose the unrealized crossing symmetries, as extra conditions, on these fixed t dispersion relations or the sum rules. This gives rise to null constraints, which can significantly strengthen the positivity bounds, capable to bound the Wilson coefficients from the below and from the above [6, 7].

In the Higgs case, the null constraints can be obtained by equating different expressions of the same Wilson coefficient in various dispersion relations. For example, the coefficients in front of the terms s^3 and s^2t in the dispersion relation of $\mathcal{M}^{1\bar{1}2\bar{2}}(s,t)$ give rise to sum rules for c_1 and c_2, as shown in Eqs. (18) and (19). On the other hand, from the dispersion relation of $\mathcal{M}^{1\bar{2}\bar{2}}(t,s)$, the sum rule obtained from the s^2t term is given by

$$-3c_1+2c_2= \left\langle\frac{(1+(-1)^\ell)\ell(1+\ell)\rho_t^t(\mu)+(-1)^\ell(-3+\ell+\ell^2)(\rho_t^s(\mu)+\rho_t^u(\mu))}{\mu^4}\right\rangle. \tag{20}$$

Plugging the sum rules Eqs. (18) and (19) into the sum rule Eq. (20), we can get one null constraint:

$$\begin{aligned} 0=\Big\langle\frac{1}{\mu^4}\{&[3-3(-1)^\ell+(-2+(-1)^\ell)\ell+(-2+(-1)^\ell)\ell^2](\rho_t^s+\rho_t^u)+\\ &(1+(-1)^\ell)\ell(1+\ell)\rho_t^t\}\Big\rangle. \end{aligned} \tag{21}$$

To get independent null constraints, we only need to extract sum rules from the dispersion relations of $\mathcal{M}^{1\bar{1}2\bar{2}}(s,t),\mathcal{M}^{1\bar{1}\bar{2}2}(t,s)$, and $\mathcal{M}^{1\bar{1}1\bar{1}}(s,t)$. If a coefficient appears in multiple sum rules, we can obtain null constraints as illustrated above. As the order of the sum rules increases, the number of independent null constraints increases, but all of these can be easily handled by a symbolic algebra system.

2.3 Nonlinear unitarity

Ref. [73] derived a set of linearized unitarity conditions that can be used to obtain two-sided bounds on generic dim-8 Wilson coefficients. These linearized unitarity conditions are explicit, simple and easy to use in a linear program. In fact, they can be easily implemented with simple `Mathematica` coding to compute the numerical bounds. In this paper, we further use stronger, nonlinear unitarity conditions, which generally lead to stronger bounds; see Appendix A.2. For the Higgs case, however, due to the high degrees of the internal symmetries, the nonlinear unitarity conditions are actually

DOI: 10.52396/JUSTC-2023-0159
JUSTC, **2024**, 54(7): 0705

equivalent to the linear ones, as we shall see in Section 4.

Recall that the full unitarity condition is $\boldsymbol{S}\boldsymbol{S}^\dagger = \boldsymbol{I}$, where $\boldsymbol{S}$ is the S-matrix and $\boldsymbol{I}$ is the corresponding identity matrix. If we restrict to a subspace of the space of all outgoing states, the reduced unitarity conditions can be written as $\hat{\boldsymbol{S}}\hat{\boldsymbol{S}}^\dagger \le \boldsymbol{I}$, where $\hat{\boldsymbol{S}}$ is the projection of $\boldsymbol{S}$ to the subspace. Splitting the projected S-matrix into an identity matrix plus a transfer matrix $\hat{\boldsymbol{T}}$: $\hat{\boldsymbol{S}} = \boldsymbol{I} + \mathrm{i}\hat{\boldsymbol{T}}$, we have $(\boldsymbol{I} - \mathrm{Im}\boldsymbol{T})^2 + (\mathrm{Re}\boldsymbol{T})^2 \le \boldsymbol{I}$. Since $(\mathrm{Re}\boldsymbol{T})^2$ is semi-positive, a weaker but simpler condition is $\boldsymbol{I} - (\boldsymbol{I} - \mathrm{Im}\boldsymbol{T})^2 \ge 0$, which is equal to the following linear matrix inequalities

$$\mathrm{Im}\boldsymbol{T} \ge 0, \qquad 2\boldsymbol{I} - \mathrm{Im}\boldsymbol{T} \ge 0. \tag{22}$$

In the scattering, angular momenta are conserved, so the above inequalities also apply to each partial waves:

$$\mathrm{Im}\boldsymbol{T}_\ell \ge 0, \qquad 2\boldsymbol{I} - \mathrm{Im}\boldsymbol{T}_\ell \ge 0. \tag{23}$$

Note that in terms of partial wave amplitudes, these unitarity conditions are highly nonlinear. For the Higgs case we have in hand, for each partial wave, $\boldsymbol{T}_\ell$ is a 16×16 matrix and the partial wave amplitudes are related to it by

$$\rho_\ell^{ijkl}(s) = \begin{cases} \boldsymbol{T}_\ell^{ijkl}(s)/2, & \text{for } i \ne j \text{ and } k \ne l; \\ \boldsymbol{T}_\ell^{ijkl}(s), & \text{for } i = j \text{ and } k = l; \\ \boldsymbol{T}_\ell^{ijkl}(s)/\sqrt{2}, & \text{for } (i \ne j \text{ and } k = l) \text{ or } (i = j \text{ and } k \ne l). \end{cases} \tag{24}$$

where the factor 2 comes from the bose symmetry.

These conditions are generically stronger than those linear unitarity conditions obtained in Ref. [73], as demonstrated in Appendix A.2 for the case of a simple bi-scalar theory. In Appendix A.1, we show how to re-derive the linear conditions of Ref. [73] from the nonlinear conditions Eq. (23).

3 Numerical implementation

In the last section, we have derived the sum rules which express the Wilson coefficients in terms of a sum of different UV spin contributions and each UV spin contribution is expressed as an integral over the UV energy scale. We do not know the exact values of the UV partial wave amplitudes, but they should satisfy the partial wave unitarity. Now, we shall numerically implement the nonlinear unitarity conditions Eq. (23) within SDPB. Additionally, the UV partial wave amplitudes should also satisfy the null constraints, which are also easy to implement with the SDPB package[76]. In this section, we shall set up the numerical method to compute the optimal bounds on the Wilson coefficients.

Our strategy is to discretize the UV scale μ, after which we are left with a finite number of the imaginary part of the UV partial wave amplitudes $\rho_\ell^s(\mu)$, $\rho_\ell^t(\mu)$, and $\rho_\ell^u(\mu)$, the decision variables in the optimization problem. Specifically, in the numerical scheme, we choose $\ell = 0, 1, \ldots, \ell_M, \ell_\infty$ and $\Lambda^2/\mu = 1/N, \ldots, 1$, where ℓ_M and N are two sufficiently large integers for the numerics to converge and a larger partial wave $\ell_\infty \gg \ell_M$ is chosen to make the numerics converge faster. For example, under the discretization, Eq. (17) becomes

$$\begin{aligned} b_1 &= \sum_\ell 16(2\ell+1)\int_{\Lambda^2}^\infty \mathrm{d}\mu \frac{\rho_\ell^s(\mu)+\rho_\ell^u(\mu)}{\mu^3} \\ &\approx \frac{1}{\Lambda^4}\sum_{\ell=0}^{\ell_\mathrm{M},\ell_\infty} 16(2\ell+1)\sum_{n=1}^N \frac{1}{N}\frac{n}{N}(\rho_{\ell,n}^s + \rho_{\ell,n}^u), \end{aligned} \tag{25}$$

where we have defined $\rho_{\ell,n}^s = \rho_\ell^s(\Lambda^2 N/n)$ and so on. Note that now b_1 is a finite, linear combination of the decision variables. The same discretization is also applied to the null constraints. The null constraints are equality constraints, and in SDPB these equality constraints can be implemented by both imposing $(...) \ge 0$ and $(...) \le 0$. With these setups, we can now propose our semi-definite program to get the bounds on the Wilson coefficients:

Decision variables

$$\rho_{\ell,n}^s,\ \rho_{\ell,n}^t,\ \rho_{\ell,n}^u \qquad \text{for } \ell = 0, 1, \ldots, \ell_\mathrm{M}, \ell_\infty \text{ and } n = 1, 2, ..., N \tag{26}$$

Maximize/Minimize

$$\sum_{I=1}^3 \alpha_I C_I, \text{ where}$$

$$C_1 = \frac{1}{\Lambda^4}\sum_{\ell=0}^{\ell_\mathrm{M},\ell_\infty} 16(2\ell+1)\sum_{n=1}^N \frac{1}{N}\frac{n}{N}\Big((1-(-1)^\ell)(\rho_{\ell,n}^s+\rho_{\ell,n}^t)+ ((-1)^\ell+1)\rho_{\ell,n}^u\Big); \tag{27}$$

$$C_2 = \frac{1}{\Lambda^4}\sum_{\ell=0}^{\ell_\mathrm{M},\ell_\infty} 16(2\ell+1)\sum_{n=1}^N \frac{1}{N}\frac{n}{N}\Big(((-1)^\ell-1)(\rho_{\ell,n}^s+\rho_{\ell,n}^u)+ ((-1)^\ell+1)\rho_{\ell,n}^t\Big); \tag{28}$$

$$C_3 = \frac{1}{\Lambda^4}\sum_{\ell=0}^{\ell_\mathrm{M},\ell_\infty} 16(2\ell+1)\sum_{n=1}^N \frac{1}{N}\frac{n}{N}\Big(((-1)^\ell+1)\rho_{\ell,n}^s+ ((-1)^\ell-1)(\rho_{\ell,n}^t-\rho_{\ell,n}^u)\Big). \tag{29}$$

Subject to

Unitarity conditions (22)

Null constraints such as (21)

α_I are constants to be chosen by the user, which specifies the direction in the Wilson coefficient space $\{C_I\}$ that one wants to bound. In practice, since some of the unitarity conditions contain constants, we can introduce an extra decision variable and use the SDPB normalization to set this variable to 1.

In this paper, we shall only present 1D and 2D bounds. For the 1D bounds, we calculate the bounds on each of C_I. To get 2D bounds, we set one of α_I to zero and use the angular optimization method to compute the boundary of the bounds. For example, to obtain the bounds on C_1 and C_2, we set $(\alpha_1, \alpha_2, \alpha_3) = (\cos\theta, \sin\theta, 0)$. For each fixed θ, we use the SDPB package to obtain a lower and an upper bound on the objective $\cos\theta C_1 + \sin\theta C_2$, each upper or lower bound delineating a half plane in the C_1-C_2 space. Doing this for a number of θ, the many half-spaces carve out a 2D boundary in the C_1-C_2 space.

DOI: 10.52396/JUSTC-2023-0159
JUSTC, 2024, 54(7): 0705

4 Bounds on dim-8 Higgs operators

In this section, we present the numerical results on the SMEFT Higgs coefficients C_1, C_2, and C_3. With the Semidefinite Program (SDP) setup in the last section, we can find both upper and lower positivity bounds on them. We will compare our results with those from Ref. [73]. The positivity bounds obtained in Ref. [73] are already often stronger than the experiments bounds and the so-called partial wave unitarity bounds. As we see below, our bounds here are even stronger. Note that the partial wave unitarity bounds are *not* positivity bounds. The partial wave unitarity bounds reply only on partial wave unitarity within the low energy EFT, and dispersion relations are not used in their derivation. In comparison, the positivity bounds① (sometimes also known as causality bounds) are built up on the dispersion relations, whose existence relies on causality of the S-matrix, and make use of the partial wave unitarity of the unknown UV theory.

In Table 1, we see that, comparing with the results in Ref. [73], labeled as "Linear", our 1D "Nonlinear" bounds are much stronger, almost by a factor of 2. Comparing to the experiments bounds and the partial wave unitarity bounds that have also been obtained in Ref. [73], which we shall not repeat here, these new results will be more useful in helping the phenomenological analysis of the collider data. We also compute the 2D positivity bounds in the C_1-C_2, C_1-C_3, and C_2-C_3 plane respectively, which are shown in Fig. 1. From these plots, we consistently see an improvement by about a factor of 3 or 4, compared to the results of Ref. [73]. Clearly, in the total 3D parameter space spanned by C_1, C_2, and C_3, the improvement factor is even greater.

Note that, in Fig. 1, we are plotting 3 two-dimensional projections of the *capped* positivity cone. This is different from the positivity cone of Ref. [74] in that the capped positivity cone now additionally has upper bounds, much like an ice cream cone; see Fig. 1 of Ref. [73] for a cartoon explanation. That is, the rays of the cone of Ref. [10] go to infinity, while the current capped cone is a set of finite-length line segments. In the two-dimensional projections of the capped positivity cone, we can still see some parts of the Ref. [10] cone. For example, in the left plot of Fig. 1, the projection of the Ref. [10] cone is given by the lines of $C_1 \geq 0$ and $C_1 + C_2 \geq 0$, which pass through the origin, and we see that this cone is now capped from the above by a smooth curve. The reason that we can now bound the cone from above is because: (i) we now have added the null constraints, which uses the information away from the forward limit; (ii) we have made fuller use of the partial wave unitarity conditions in the UV. For more details about this, readers are referred to Ref. [73].

Table 1. Comparison of positivity bounds on individual coefficients c_I from the linear and nonlinear unitarity conditions. Here, the "Linear2" and "Nonlinear" results are our results in this paper obtained using linear and nonlinear unitarity conditions respectively, while the "Linear" results are from Ref. [73] using linear unitarity conditions but without using full Higgs symmetries. In this table, the numerical parameters are $N = 10$ and $\ell_M = 20$, and 42 null constraints are used.

	$\bar{C}_1 = C_1\Lambda^4/(4\pi)^2$		$\bar{C}_2 = C_2\Lambda^4/(4\pi)^2$		$\bar{C}_3 = C_3\Lambda^4/(4\pi)^2$	
	lower	upper	lower	upper	lower	upper
Linear	−0.130	0.774	0	0.638	−0.508	0.408
Linear2	−0.086	0.467	0	0.378	−0.387	0.167
Nonlinear	−0.086	0.467	0	0.378	−0.387	0.167

① We emphasize that, in this paper, we have broaden the definition of positivity bounds, in that we also refer to the bounds obtained by using the non-positivity part of the unitarity conditions as positivity bounds.

In Table 1 and Fig. 1, the "Linear2" bounds are the positivity bounds that can be obtained with the linear unitarity conditions of Ref. [73] but with all the symmetries of the SMEFT Higgs included. As it happens, these "Linear2" positivity bounds are numerically the same as our "Nonlinear" bounds. This is coincidental for the case of the SMEFT Higgs, due to the presence of strong internal symmetries. To see why this happens, let us compute the eigenvalues of the matrices $\mathrm{Im}\boldsymbol{T}_\ell$ and $2\boldsymbol{I} - \mathrm{Im}\boldsymbol{T}_\ell$, which are given respectively

$$\begin{aligned}&\text{Distinct eigenvalues of } \mathrm{Im}\boldsymbol{T}_\ell:\\ &-2(-1+(-1)^\ell)\rho_\ell^t, (1+(-1)^\ell)\rho_\ell^t, 2(1+(-1)^\ell)\rho_\ell^t, 2(-1+(-1)^\ell)\rho_\ell^u,\\ &2(1+(-1)^\ell)\rho_\ell^u, 2(-1+(-1)^\ell)(2\rho_\ell^s+\rho_\ell^u), 2(1+(-1)^\ell)(2\rho_\ell^s+\rho_\ell^u),\end{aligned} \tag{30}$$

$$\begin{aligned}&\text{Distinct eigenvalues of } (2\boldsymbol{I}-\mathrm{Im}\boldsymbol{T}_\ell):\\ &2(1-\rho_\ell^t+(-1)^\ell\rho_\ell^t), -2(-1+\rho_\ell^t+(-1)^\ell\rho_\ell^t), 2-\rho_\ell^t-(-1)^\ell\rho_\ell^t,\\ &-2(-1-\rho_\ell^u+(-1)^\ell\rho_\ell^u), -2(-1-2\rho_\ell^s+2(-1)^\ell\rho_\ell^s-\rho_\ell^u+(-1)^\ell\rho_\ell^u),\\ &-2(-1+\rho_\ell^u+(-1)^\ell\rho_\ell^u), -2(-1+2\rho_\ell^s+2(-1)^\ell\rho_\ell^s+\rho_\ell^u+(-1)^\ell\rho_\ell^u).\end{aligned} \tag{31}$$

The semi-positive definiteness of $\mathrm{Im}\boldsymbol{T}_\ell$ and $2\boldsymbol{I}-\mathrm{Im}\boldsymbol{T}_\ell$ are just the semi-positivity of these eigenvalues. Remembering Eq. (9) and the relation $a_\ell^{ijkl}(s) = (-1)^\ell a_\ell^{ijlk}(s)$, it is easy to see that the positivity of these eigenvalues exactly give rise to the linear unitarity conditions for the SMEFT Higgs.

Nevertheless, the nonlinear unitarity conditions are in general stronger than the linear unitarity conditions derived in Appendix A.1. In Appendix A.2, as a simple example, we show that in a generic $\mathbb{Z}_2$ bi-scalar theory, the nonlinear bounds are indeed stronger than the linear bounds.

Finally, we would like to point out that the convergences of our numerically results are excellent. To see this, in Fig. 2, we plot how the 1D bounds varies with the number of null constraints used. In the above numerical results, we truncated the UV scales with $N = 10$ and the UV spins with $\ell_M = 20$, and we find that it is convenient to choose $\ell_\infty = 100$. With this numerical setup, the computation of a single half-space bound uses about 110 CPU hours. As N increases, the positivity bounds become weaker, while the bounds becomes tighter as ℓ_M increases. In Fig. 3, we see that the results are quite stable against increasing the values of N and ℓ_M.

5 Summary

Positivity bounds are a set of highly restrictive conditions on the low-energy Wilson coefficients that have yet to be fully appreciated by the wider particle phenomenological and experimental communities. Although the formalism of positivity bounds itself is still under active development, highly constraining results are already available and straightforward to use. Here we take the Higgs scattering in the SMEFT as an

DOI: 10.52396/JUSTC-2023-0159
JUSTC, **2024**, 54(7): 0705

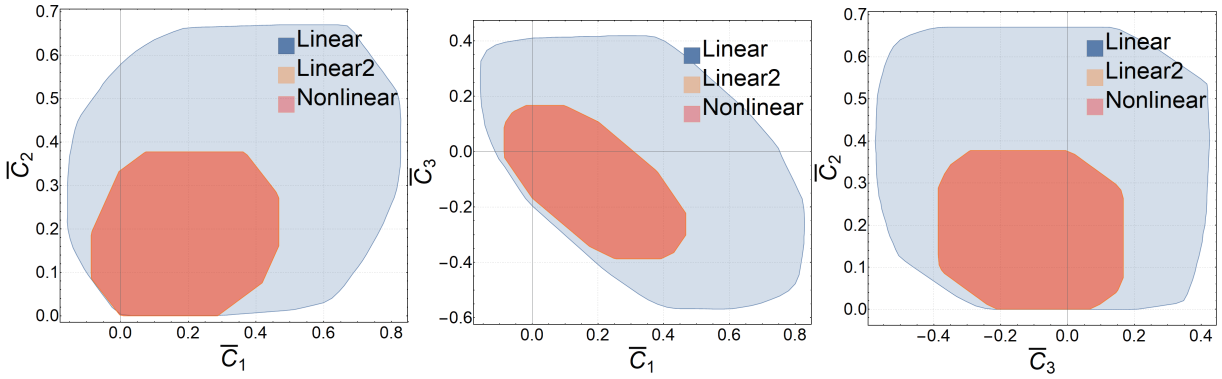

Fig. 1. Positivity regions in the 2D subspaces of C_1, C_2, and C_3 by using linear and nonlinear unitarity conditions. Here, $\bar{C}_i = C_i\Lambda^4/(4\pi)^2$. The orange and red regions are the results of the current paper using linear and nonlinear unitarity conditions respectively, while the blue region are from Ref. [24], which uses linear unitarity conditions but without using full Higgs symmetries. The orange and red regions are the same. We choose $N = 10, \ell_M = 20$ and use 42 null constraints.

Table 2. Bounds on $g^a_{1,0}$, $g^b_{2,0}$, and $g^a_{1,0}+g^b_{2,0}$, using linear and nonlinear unitarity conditions separately. Here we choose $N = 20, \ell_M = 30$.

	$\bar{g}^a_{1,0} = g^a_{1,0}\Lambda^4/(4\pi)^2$		$\bar{g}^b_{2,0} = g^b_{2,0}\Lambda^4/(4\pi)^2$		$\bar{g}^a_{1,0}+\bar{g}^b_{2,0}$	
	lower	upper	lower	upper	lower	upper
Linear	0	0.798	−0.330	0.614	−0.326	1.412
Nonlinear	0	0.798	−0.330	0.614	−0.172	1.176

example to illustrate how to numerically compute optimal, two-sided positivity bounds on ths dimension-8 Wilson coefficients. While the SMEFT formalism is generic, we assume that the SMEFT is weakly coupled below the EFT cutoff but may be strongly coupled in the UV. The formalism presented can be easily generalized to other sectors of the SMEFT, which is left for future work.

In this paper, we have improved the existing positivity bounds on the SMEFT Higgs by applying nonlinear unitarity conditions to the UV amplitude or spectral functions and by leveraging the full internal symmetries of the Higgs scattering. While the previous bounds can be obtained by simple `Mathematica` coding with linear programming, our new res-

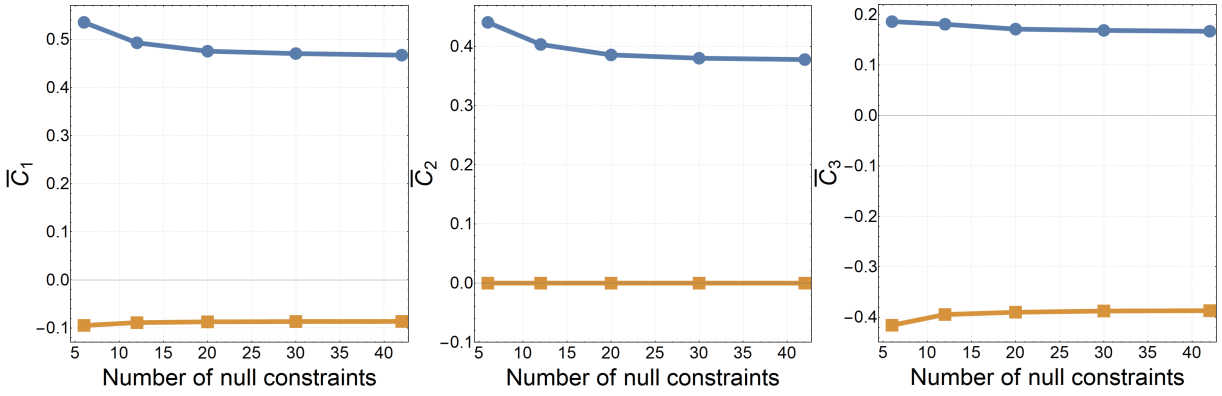

Fig. 2. Convergence of positivity (upper and lower) bounds with the number of null constraint. We choose $N = 10, \ell_M = 20$.

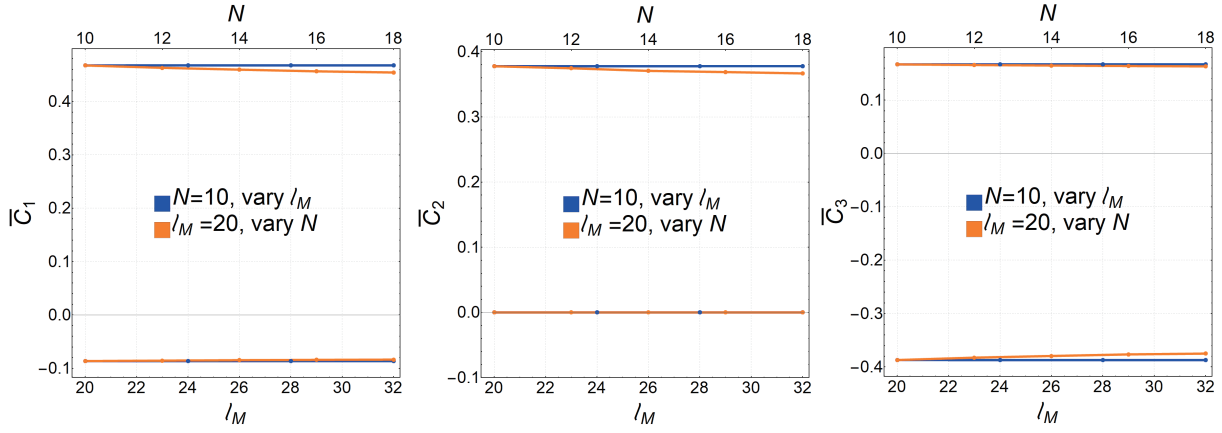

Fig. 3. Convergence of positivity (upper and lower) bounds with the numerical truncations ℓ_M and N. Here $\bar{C}_i = C_i\Lambda^4/(4\pi)^2$. 42 null constraints are used.

DOI: 10.52396/JUSTC-2023-0159
JUSTC, **2024**, 54(7): 0705

ults make use of the SDPB package, which can solve various field-theoretical semi-definite programs efficiently and highly accurately. We see that the new bounds are significantly stronger.

We have found that, in the Higgs case, the robust internal symmetries imply that the linear UV unitarity conditions used in Ref. [73] are actually tantamount to the nonlinear unitarity conditions. However, including the full internal symmetries does lead to tighter positivity bounds than the previous ones. As these new bounds are stronger than the current experimental bounds and the partial wave unitarity bounds, they will be useful in analyzing the current and upcoming phenomenological data for dimension-8 operators. These bounds may also be used to test the fundamental principles of quantum field theory or rule out UV particles from the collider data along the lines of Refs. [54, 63].

In general, the nonlinear unitarity conditions are of course more stringent. To demonstrate that the nonlinear unitarity conditions generally give rise to stronger bounds, we have calculated the two-sided positivity bounds for $\mathbb{Z}_2$ bi-scalar theory, a theory with two real scalar fields endowed with the reflection symmetry $\varphi_i \to -\varphi_i$, $i = 1,2$. Nevertheless, we see that the linear unitarity conditions already give rise to bounds that are close to the bounds from the nonlinear conditions.

Acknowledgements

This work was supported by the Fundamental Research Funds for the Central Universities (WK2030000036) and the National Natural Science Foundation of China (12075233). We thank Yue-Zhou Li, Shi-Lin Wan, Tong Wu, and Guo-Dong Zhang for helpful discussions.

Conflict of Interest

There is no conflict of interest to report.

Biographies

Dong-Yu Hong is currently a Ph.D. student at the University of Science and Technology of China. His research mainly focuses on positivity bounds in effective field theories.

Shuang-Yong Zhou is currently a Professor of Physics at the University of Science and Technology of China. He completed his Ph.D. at the University of Nottingham and subsequently held postdoctoral positions at SISSA in Trieste, Case Western Reserve University, and Imperial College London. His current research interests include S-matrix bootstrap/positivity bounds in effective field theories and their applications in particle physics and gravitational theories, as well as non-topological solitons and non-perturbative field simulations.

References

[1] Adams A, Arkani-Hamed N, Dubovsky S, et al. Causality, analyticity and an IR obstruction to UV completion. *Journal of High Energy Physics*, **2006**, *2006*: 014.
[2] de Rham C, Melville S, Tolley A J, et al. Positivity bounds for scalar field theories. *Physical Review D*, **2017**, *96*: 081702.
[3] de Rham C, Melville S, Tolley A J, et al. UV complete me: Positivity bounds for particles with spin. *Journal of High Energy Physics*, **2018**, *2018*: 11.
[4] Arkani-Hamed N, Huang T C, Huang Y T. The EFT-hedron. *Journal of High Energy Physics*, **2021**, *2021*: 259.
[5] Bellazzini B, Miró J E, Rattazzi R, et al. Positive moments for scattering amplitudes. *Physical Review D*, **2021**, *104*: 036006.
[6] Tolley A J, Wang Z Y, Zhou S Y. New positivity bounds from full crossing symmetry. *Journal of High Energy Physics*, **2021**, *2021*: 255.
[7] Caron-Huot S, Van Duong V. Extremal effective field theories. *Journal of High Energy Physics*, **2021**, *2021*: 280.
[8] Chiang L Y, Huang Y T, Li W, et al. Into the EFThedron and UV constraints from IR consistency. *Journal of High Energy Physics*, **2022**, *2021*: 63.
[9] Sinha A, Zahed A. Crossing symmetric dispersion relations in quantum field theories. *Physical Review Letters*, **2021**, *126*: 181601.
[10] Zhang C, Zhou S Y. Convex geometry perspective on the (standard model) effective field theory space. *Physical Review Letters*, **2020**, *125*: 201601.
[11] Li X, Xu H, Yang C, et al. Positivity in multifield effective field theories. *Physical Review Letters*, **2021**, *127*: 121601.
[12] Bellazzini B, Martucci L, Torre R. Symmetries, sum rules and constraints on effective field theories. *Journal of High Energy Physics*, **2014**, *2014*: 100.
[13] Bellazzini B. Softness and amplitudes' positivity for spinning particles. *Journal of High Energy Physics*, **2017**, *2017*: 34.
[14] Bern Z, Kosmopoulos D, Zhiboedov A. Gravitational effective field theory islands, low-spin dominance, and the four-graviton amplitude. *Journal of Physics A:Mathematical and Theoretical*, **2021**, *54*: 344002.
[15] Alberte L, de Rham C, Jaitly S, et al. Positivity bounds and the massless spin-2 pole. *Physical Review D*, **2020**, *102*: 125023.
[16] Tokuda J, Aoki K, Hirano S. Gravitational positivity bounds. *Journal of High Energy Physics,*, **2020**, *2020*: 54.
[17] Caron-Huot S, Mazáč D, Rastelli L, et al. Sharp boundaries for the swampland. *Journal of High Energy Physics*, **2021**, *2021*: 110.
[18] Grall T, Melville S. Positivity bounds without boosts: New constraints on low energy effective field theories from the UV. *Physical Review D*, **2022**, *105*: L121301.
[19] Du Z Z, Zhang C, Zhou S Y. Triple crossing positivity bounds for multi-field theories. *Journal of High Energy Physics*, **2021**, *2021*: 115.
[20] Alberte L, de Rham C, Jaitly S, et al. Reverse bootstrapping: IR lessons for UV physics. *Physical Review Letters*, **2022**, *128*: 051602.
[21] Bellazzini B, Riembau M, Riva F. IR side of positivity bounds. *Physical Review D*, **2022**, *106*: 105008.
[22] Dutta Chowdhury S, Ghosh K, Haldar P, et al. Crossing symmetric spinning S-matrix bootstrap: EFT bounds. *SciPost Physics*, **2022**, *13*: 51.
[23] Chiang L Y, Huang Y T, Rodina L, et al. De-projecting the EFThedron. *Journal of High Energy Physics*, **2024**, *2024*: 102.
[24] Caron-Huot S, Li Y Z, Parra-Martinez J, et al. Causality constraints on corrections to Einstein gravity. *Journal of High Energy Physics*, **2023**, *2023*: 122.
[25] Caron-Huot S, Li Y Z, Parra-Martinez J, et al. Graviton partial waves and causality in higher dimensions. *Physical Review D*, **2023**, *108*: 026007.
[26] Henriksson J, McPeak B, Russo F, et al. Bounding violations of the weak gravity conjecture. *Journal of High Energy Physics*, **2022**, *2022*: 184.
[27] Li-Yuan Chiang, Yu-tin Huang, Wei Li, Laurentiu Rodina, and He-Chen Weng. (Non)-projective bounds on gravitational EFT. arXiv: 2201. 07177, **2022**.
[28] Albert J, Rastelli L. Bootstrapping pions at large N. *Journal of High*

DOI: 10.52396/JUSTC-2023-0159
JUSTC, **2024**, 54(7): 0705

Energy Physics, **2022**, *2022*: 151.
[29] Carrillo González M, de Rham C, Jaitly S, et al. Positivity-causality competition: A road to ultimate EFT consistency constraints. *Journal of High Energy Physics*, **2024**, *2024*: 146.
[30] Hong D Y, Wang Z H, Zhou S Y. Causality bounds on scalar-tensor EFTs. *Journal of High Energy Physics*, **2023**, *2023*: 135.
[31] Li Y Z. Effective field theory bootstrap, large-N χPT and holographic QCD. *Journal of High Energy Physics*, **2024**, *2024*: 72.
[32] Paulos M F, Penedones J, Toledo J, et al. The S-matrix bootstrap II: Two dimensional amplitudes. *Journal of High Energy Physics*, **2017**, *2017*: 143.
[33] Paulos M F, Penedones J, Toledo J, et al. The S-matrix bootstrap. *Part III:Higher dimensional amplitudes. Journal of High Energy Physics*, **2019**, *2019*: 40.
[34] He Y, Irrgang A, Kruczenski M. A note on the S-matrix bootstrap for the 2d O(N) bosonic model. *Journal of High Energy Physics*, **2018**, *2018*: 93.
[35] He Y, Kruczenski M. S-matrix bootstrap in 3+1 dimensions: Regularization and dual convex problem. *Journal of High Energy Physics*, **2021**, *2021*: 125.
[36] Karateev D, Kuhn S, Penedones J. Bootstrapping massive quantum field theories. *Journal of High Energy Physics*, **2020**, *2020*: 35.
[37] Guerrieri A L, Penedones J, Vieira P. S-matrix bootstrap for effective field theories: Massless pions. *Journal of High Energy Physics*, **2021**, *2021*: 88.
[38] Kruczenski M, Murali H. The R-matrix bootstrap for the 2d O(N) bosonic model with a boundary. *Journal of High Energy Physics*, **2021**, *2021*: 97.
[39] Guerrieri A, Sever A. Rigorous bounds on the analytic *S* matrix . *Physical Review Letters*, **2021**, *127*: 251601.
[40] Guerrieri A, Penedones J, Vieira P. Where is string theory in the space of scattering amplitudes. *Physical Review Letters*, **2021**, *127*: 081601.
[41] Albert J, Rastelli L. Bootstrapping pions at large *N*. Part II: background gauge fields and the chiral anomaly. arXiv: 2307. 01246, **2023**.
[42] Acanfora F, Guerrieri A, Häring K, et al. Bounds on scattering of neutral Goldstones. *Journal of High Energy Physics*, **2024**, *2024*: 28.
[43] Miró J E, Guerrieri A, Gumus M A. Extremal Higgs couplings. arXiv: 2311. 09283, **2023**.
[44] de Rham C, Kundu S, Reece M, et al. Snowmass white paper: UV constraints on IR physics. arXiv: 2203. 06805, **2022**.
[45] Zhang C, Zhou S Y. Positivity bounds on vector boson scattering at the LHC. *Physical Review D*, **2019**, *100*: 095003.
[46] Bi Q, Zhang C, Zhou S Y. Positivity constraints on aQGC: Carving out the physical parameter space. *Journal of High Energy Physics*, **2019**, *2019*: 137.
[47] Bellazzini B, Riva F. New phenomenological and theoretical perspective on anomalous ZZ and Zγ processes. *Physical Review D*, **2018**, *98*: 095021.
[48] Remmen G N, Rodd N L. Consistency of the standard model effective field theory. *Journal of High Energy Physics*, **2019**, *2019*: 32.
[49] Yamashita K, Zhang C, Zhou S Y. Elastic positivity vs extremal positivity bounds in SMEFT: A case study in transversal electroweak gauge-boson scatterings. *Journal of High Energy Physics*, **2021**, *2021*: 95.
[50] Trott T. Causality, unitarity and symmetry in effective field theory. *Journal of High Energy Physics*, **2021**, *2021*: 143.
[51] Remmen G N, Rodd N L. Flavor constraints from unitarity and analyticity. *Physical Review Letters*, **2020**, *125*: 081601.
[52] Remmen G N, Rodd N L. Signs, spin, SMEFT: Sum rules at dimension six. *Physical Review D*, **2022**, *105*: 036006.
[53] Gu J, Wang L T. Sum rules in the standard model effective field theory from helicity amplitudes. *Journal of High Energy Physics*, **2021**, *2021*: 149.
[54] Fuks B, Liu Y, Zhang C, et al. Positivity in electron-positron scattering: Testing the axiomatic quantum field theory principles and probing the existence of UV states. *Chinese Physics C*, **2021**, *45*: 023108.
[55] Gu J, Wang L T, Zhang C. Unambiguously testing positivity at lepton colliders. *Physical Review Letters*, **2022**, *129*: 011805.
[56] Bonnefoy Q, Gendy E, Grojean C. Positivity bounds onminimal flavor violation. *Journal of High Energy Physics*, **2021**, *2021*: 115.
[57] Davighi J, Melville S, You T. Natural selection rules: New positivity bounds for massive spinning particles. *Journal of High Energy Physics*, **2022**, *2022*: 167.
[58] Chala M, Santiago J. Positivity bounds in the standard model effective field theory beyond tree level. *Physical Review D*, **2022**, *105*: L111901.
[59] Zhang C. SMEFTs living on the edge: Determining the UV theories from positivity and extremality. *Journal of High Energy Physics*, **2022**, *2022*: 96.
[60] Ghosh D, Sharma R, Ullah F. Amplitude's positivity *vs.* subluminality: Causality and unitarity constraints on dimension 6 & 8 gluonic operators in the SMEFT. *Journal of High Energy Physics*, **2023**, *2023*: 199.
[61] Remmen G N, Rodd N L. Spinning sum rules for the dimension-six SMEFT. *Journal of High Energy Physics*, **2022**, *2022*: 30.
[62] Li X, Zhou S. Origin of neutrino masses on the convex cone of positivity bounds. *Physical Review D*, **2023**, *107*: L031902.
[63] Li X, Mimasu K, Yamashita K, et al. Moments for positivity: Using Drell-Yan data to test positivity bounds and reverse-engineer new physics. *Journal of High Energy Physics*, **2022**, *2022*: 107.
[64] Li X. Positivity bounds at one-loop level: The Higgs sector. *Journal of High Energy Physics*, **2023**, *2023*: 230.
[65] Altmannshofer W, Gori S, Lehmann B V, et al. UV physics from IR features: New prospects from top flavor violation. *Physical Review D*, **2023**, *107*: 095025.
[66] Davighi J, Melville S, Mimasu K, et al. Positivity and the electroweak hierarchy. *Physical Review D*, **2024**, *109*: 033009.
[67] Ellis J, Mimasu K, Zampedri F. Dimension-8 SMEFT analysis of minimal scalar field extensions of the Standard Model. *Journal of High Energy Physics*, **2023**, *2023*: 51.
[68] Chala M, Li X. Positivity restrictions on the mixing of dimension-eight SMEFT operators. *Physical Review D*, **2024**, *109*: 065015.
[69] Gu J, Shu C. Probing positivity at the LHC with exclusive photon-fusion processes. *Journal of High Energy Physics*, **2024**, *2024*: 183.
[70] Li H L, Ren Z, Shu J, et al. Complete set of dimension-eight operators in the standard model effective field theory. *Physical Review D*, **2021**, *104*: 015026.
[71] Murphy C W. Dimension-8 operators in the Standard Model Effective Field Theory. *Journal of High Energy Physics*, **2020**, *2020*: 174.
[72] Vecchi L. Causal *vs.* analytic constraints on anomalous quartic gauge couplings. *Journal of High Energy Physics*, **2007**, *2007*: 54.
[73] Chen Q, Mimasu K, Wu T A, et al. Capping the positivity cone: Dimension-8 Higgs operators in the SMEFT. *Journal of High Energy Physics*, **2024**, *2024*: 180.
[74] Froissart M. Asymptotic behavior and subtractions in the mandelstam representation. *Physical Review*, **1961**, *123*: 1053–1057.
[75] Martin A. Unitarity and high-energy behavior of scattering amplitudes. *Physical Review*, **1963**, *129*: 1432–1436.
[76] Landry W, Simmons-Duffin D. Scaling the semidefinite program

DOI: 10.52396/JUSTC-2023-0159
JUSTC, **2024**, 54(7): 0705

solver SDPB. arXiv: 1909. 09745, **2019**.

Appendix

A.1 Linear unitarity from nonlinear unitarity

In this Appendix, we re-derive the linear unitarity conditions of Ref. [24] from the linear matrix inequalities (23), which are non-linear in terms of the partial wave amplitudes. In this appendix only, we choose the physical momenta for all the particles, not using the all in-going convention.

Firstly, we derive the linear unitarity conditions on ρ_ℓ^{iiii} and ρ_ℓ^{iijj} with $i \neq j$. Let us focus on the following sub-matrix, which is the smallest sub-matrix containing ρ_ℓ^{iiii} and ρ_ℓ^{iijj}.

$$\begin{pmatrix} \rho_\ell^{iiii} & \rho_\ell^{iijj} \\ \rho_\ell^{iijj} & \rho_\ell^{jjjj} \end{pmatrix}. \tag{A1}$$

If a Hermitian matrix $\boldsymbol{M}$ is positive semi-definite, then its principal sub-matrices are also positive semi-definite. So $\mathrm{Im}\boldsymbol{T} \geq 0$ and $2\boldsymbol{I} - \mathrm{Im}\boldsymbol{T} \geq 0$ implies that we must have

$$\begin{pmatrix} \rho_\ell^{iiii} & \rho_\ell^{iijj} \\ \rho_\ell^{iijj} & \rho_\ell^{jjjj} \end{pmatrix} \geq 0, \quad \begin{pmatrix} 2-\rho_\ell^{iiii} & -\rho_\ell^{iijj} \\ -\rho_\ell^{iijj} & 2-\rho_\ell^{jjjj} \end{pmatrix} \geq 0. \tag{A2}$$

It is easy to see that these matrix inequalities imply

$$0 \leq \rho_\ell^{iiii} \leq 2, \ \rho_\ell^{iiii}\rho_\ell^{jjjj} \geq (\rho_\ell^{iijj})^2, \ (2-\rho_\ell^{iiii})(2-\rho_\ell^{jjjj}) \geq (\rho_\ell^{iijj})^2. \tag{A3}$$

Combining these with the arithmetic-geometric mean inequality, we immediately get

$$\frac{\rho_\ell^{iiii}+\rho_\ell^{jjjj}}{2} \geq |\rho_\ell^{iijj}|, \quad \frac{4-\rho_\ell^{iiii}-\rho_\ell^{jjjj}}{2} \geq |\rho_\ell^{iijj}|. \tag{A4}$$

Next, we will derive the linear unitarity conditions on ρ_ℓ^{ijij},ρ_ℓ^{klkl} and ρ_ℓ^{ijkl}, where $i \neq j \neq k \neq l$. This time we consider the following sub-matrix of $\mathrm{Im}\mathbb{T}$, which only contains the two-particle states ij, ji, kl, lk,

$$\begin{pmatrix} 2\rho_\ell^{ijij} & 2\rho_\ell^{ijji} & 2\rho_\ell^{ijkl} & 2\rho_\ell^{ijlk} \\ 2\rho_\ell^{iiij} & 2\rho_\ell^{iiji} & 2\rho_\ell^{iikl} & 2\rho_\ell^{iilk} \\ 2\rho_\ell^{klij} & 2\rho_\ell^{klji} & 2\rho_\ell^{klkl} & 2\rho_\ell^{kllk} \\ 2\rho_\ell^{lkij} & 2\rho_\ell^{lkji} & 2\rho_\ell^{lkkl} & 2\rho_\ell^{lklk} \end{pmatrix} = \begin{pmatrix} 2\rho_\ell^{ijij} & 2\rho_\ell^{ijji} & 2\rho_\ell^{ijkl} & 2\rho_\ell^{ijlk} \\ 2\rho_\ell^{ijji} & 2\rho_\ell^{ijij} & 2\rho_\ell^{ijlk} & 2\rho_\ell^{ijkl} \\ 2\rho_\ell^{ijkl} & 2\rho_\ell^{ijlk} & 2\rho_\ell^{klkl} & 2\rho_\ell^{kllk} \\ 2\rho_\ell^{ijlk} & 2\rho_\ell^{ijkl} & 2\rho_\ell^{kllk} & 2\rho_\ell^{klkl} \end{pmatrix}. \tag{A5}$$

where the right hand side of the equality is obtained by using the relation $\rho_\ell^{ijkl} = (-1)^\ell \rho_\ell^{ijlk}$. If we further restrict to the upper-left 2×2 sub-matrix, which is a principal minor of $\mathrm{Im}\boldsymbol{T}$, (23) implies that

$$0 \leq \rho_\ell^{ijij} \leq \frac{1}{2}, \tag{A6}$$

Similarly, if we consider the central 2×2 sub-matrix, $\mathrm{Im}\boldsymbol{T} \geq 0$ leads to

$$\frac{\rho_\ell^{ijij}+\rho_\ell^{klkl}}{2} \geq \sqrt{\rho_\ell^{ijij}\rho_\ell^{klkl}} \geq |\rho_\ell^{ijkl}|. \tag{A7}$$

Furthermore, the second equation in (23) implies that the determinant of the full sub-matrix (A5) is positive semi-definite

$$\begin{aligned} 0 \leq \mathrm{Det}&\begin{pmatrix} 2-2\rho_\ell^{ijij} & -2\rho_\ell^{ijji} & -2\rho_\ell^{ijkl} & -2\rho_\ell^{ijlk} \\ -2\rho_\ell^{ijji} & 2-2\rho_\ell^{ijij} & -2\rho_\ell^{ijlk} & -2\rho_\ell^{ijkl} \\ -2\rho_\ell^{ijkl} & -2\rho_\ell^{ijlk} & 2-2\rho_\ell^{klkl} & -2\rho_\ell^{kllk} \\ -2\rho_\ell^{ijlk} & -2\rho_\ell^{ijkl} & -2\rho_\ell^{kllk} & 2-2\rho_\ell^{klkl} \end{pmatrix} \\ &= 16 - 32\rho_\ell^{ijij} - 32\rho_\ell^{klkl} + 64\rho_\ell^{ijij}\rho_\ell^{klkl} - 64(\rho_\ell^{ijkl})^2 \\ &\leq 16 - 32\rho_\ell^{ijij} - 32\rho_\ell^{klkl} + 16(\rho_\ell^{ijij}+\rho_\ell^{klkl})^2 - 64(\rho_\ell^{ijkl})^2 \\ &= 16(1-\rho_\ell^{ijij}-\rho_\ell^{klkl})^2 - 64(\rho_\ell^{ijkl})^2, \end{aligned} \tag{A8}$$

which in turn leads to

$$|\rho_\ell^{ijkl}| \leq \frac{1-\rho_\ell^{ijij}-\rho_\ell^{klkl}}{2}. \tag{A9}$$

For the linear inequality $|(\rho_\ell^{iijj}+\rho_\ell^{kkll}) \pm (\rho_\ell^{iikk}+\rho_\ell^{jjll})| \leq 2$, it is not straightforward to see from the nonlinear conditions $\mathrm{Im}\boldsymbol{T} \geq 0$ and $2\boldsymbol{I} - \mathrm{Im}\boldsymbol{T} \geq 0$. For the Higgs case, with all the internal symmetries included, this inequality actually does not lead to extra

DOI: 10.52396/JUSTC-2023-0159
JUSTC, **2024**, 54(7): 0705

constraints. Thus, we see that the nonlinear unitarity conditions we use in this paper are stronger than the linear unitarity conditions used in Ref. [24].

A.2 Bounds on $\mathbb{Z}_2$ bi-scalar theory

In this appendix, we take the $\mathbb{Z}_2$ bi-scalar theory as an example to illustrate that generically, in the absence of strong symmetries, the nonlinear unitarity conditions, as expected, do lead to stronger positivity bounds than the linear unitarity conditions of Ref. [24].

By $\mathbb{Z}_2$ bi-scalar theory, we mean a theory with two real scalar fields, φ_1 and φ_2, where the theory is invariant under the $\mathbb{Z}_2$ symmetry $\varphi_i \to -\varphi_i$, $i = 1,2$. It is easy to see that in $\mathbb{Z}_2$ bi-scalar theory, 2-to-2 amplitudes $\mathcal{A}^{1112}$ and $\mathcal{A}^{2221}$ vanish, the same also applicable to the amplitudes with the cyclic permutations of $\mathcal{A}^{1112}$ and $\mathcal{A}^{2221}$. Taking these into account, we can write the amplitudes as follows

$$\mathcal{A}^{1111}(s,t) = g^a_{0,0} + g^a_{1,0}(s^2+t^2+u^2) + g^a_{0,1}stu + \cdots \tag{A10}$$

$$\mathcal{A}^{1122}(s,t) = g^b_{0,0} + g^b_{1,0}s + g^b_{0,1}tu + g^b_{2,0}s^2 + g^b_{1,1}stu + g^b_{3,0}s^3 + \cdots \tag{A11}$$

$$\mathcal{A}^{2222}(s,t) = g^c_{0,0} + g^c_{1,0}(s^2+t^2+u^2) + g^c_{0,1}stu + \cdots \tag{A12}$$

and the nonlinear unitarity conditions are given by

$$\begin{pmatrix} \rho_\ell^{1111} & \rho_\ell^{1122} & 0 & 0 \\ \rho_\ell^{2211} & \rho_\ell^{2222} & 0 & 0 \\ 0 & 0 & 2\rho_\ell^{1212} & 2\rho_\ell^{1221} \\ 0 & 0 & 2\rho_\ell^{2112} & 2\rho_\ell^{2121} \end{pmatrix} \geq 0, \tag{A13}$$

$$\begin{pmatrix} 2-\rho_\ell^{1111} & -\rho_\ell^{1122} & 0 & 0 \\ -\rho_\ell^{2211} & 2-\rho_\ell^{2222} & 0 & 0 \\ 0 & 0 & 2-2\rho_\ell^{1212} & -2\rho_\ell^{1221} \\ 0 & 0 & -2\rho_\ell^{2112} & 2-2\rho_\ell^{2121} \end{pmatrix} \geq 0, \tag{A14}$$

which is equivalent to

$$0 \leq \rho_\ell^{1111} \leq 2, \qquad 0 \leq \rho_\ell^{2222} \leq 2, \qquad 0 \leq \rho_\ell^{1212} \leq \frac{1}{2}, \tag{A15}$$

$$\rho_\ell^{1111}\rho_\ell^{2222} \geq (\rho_\ell^{1122})^2, \qquad (2-\rho_\ell^{1111})(2-\rho_\ell^{2222}) \geq (\rho_\ell^{1122})^2. \tag{A16}$$

The null constraints are just the same as Refs. [24, 34]. For our purposes, we will only calculate the positivity bounds on the following two coefficients as well as their sum as an example:

$$g^a_{1,0} = \left\langle \frac{\rho_\ell^{1111}(\mu)}{\mu^3} \right\rangle, \tag{A17}$$

$$g^b_{2,0} = \left\langle \frac{\rho_\ell^{1122}(\mu) + (-1)^\ell \rho_\ell^{1212}(\mu)}{\mu^3} \right\rangle. \tag{A18}$$

For the numerical optimization scheme, we essentially follow the same scheme as the Higgs case in the main text. With similar notations, the SDP we need to solve is given by:

Decision variables

$$\rho^{1111}_{\ell,n}, \rho^{2222}_{\ell,n}, \rho^{1122}_{\ell,n}, \rho^{1212}_{\ell,n} \quad \text{for } \ell = 0,1,\ldots,\ell_{\rm M},\ell_\infty \text{ and } n = 1,2,...,N \tag{A19}$$

Maximize/Minimize

$$g^a_{1,0} = \frac{1}{\Lambda^4}\sum_{\ell=0}^{\ell_{\rm M},\ell_\infty} 16(2\ell+1)\sum_{n=1}^{N}\frac{1}{N}\frac{n}{N}\rho^{1111}_{\ell,n} \tag{A20}$$

$$g^b_{2,0} = \frac{1}{\Lambda^4}\sum_{\ell=0}^{\ell_{\rm M},\ell_\infty} 16(2\ell+1)\sum_{n=1}^{N}\frac{1}{N}\frac{n}{N}(\rho^{1122}_{\ell,n} + (-1)^\ell\rho^{1212}_{\ell,n}) \tag{A21}$$

DOI: 10.52396/JUSTC-2023-0159
JUSTC, **2024**, 54(7): 0705

$$g^a_{1,0}+g^b_{2,0}=\frac{1}{\Lambda^4}\sum_{\ell=0}^{\ell_{\rm M},\ell_\infty}16(2\ell+1)\sum_{n=1}^{N}\frac{1}{N}\frac{n}{N}(\rho^{1111}_{\ell,n}+\rho^{1122}_{\ell,n}+(-1)^\ell\rho^{1212}_{\ell,n}) \tag{A22}$$

Subject to

Unitarity conditions (A15) – (A16)

Null constraints

As for the corresponding linear unitarity conditions, it is easy to get them from (A16) using the arithmetic-geometric mean inequality:

$$\frac{\rho^{1111}_\ell+\rho^{2222}_\ell}{2}\geq|\rho^{1122}_\ell|,\quad \frac{4-\rho^{1111}_\ell-\rho^{2222}_\ell}{2}\geq|\rho^{1122}_\ell|. \tag{A23}$$

To obtain the positivity bounds using linear unitarity conditions, we only need to replace the nonlinear unitarity conditions (A16) by (A23) in the above SDP.

Note that the equality of the arithmetic-geometric mean inequality can be saturated when $\rho^{1111}_\ell=\rho^{2222}_\ell$. Thus, if we have $\rho^{1111}_\ell=\rho^{2222}_\ell$ at (the boundaries of) the positivity bounds, the bounds from the linear unitarity conditions will be the same as those from the nonlinear unitarity conditions. It is for this reason that for a double $\mathbb{Z}_2$ bi-scalar theory where there is an additional $\mathbb{Z}_2$ symmetry $\varphi_1\leftrightarrow\varphi_2$, the positivity bounds from the linear unitarity conditions are the same as those from the nonlinear unitarity conditions, which we have verified numerically.

We present the bounds on $g^a_{1,0}$, $g^b_{2,0}$, and $g^a_{1,0}+g^b_{2,0}$ in Table 2. We observe that the linear and nonlinear bounds on $g^a_{1,0}+g^b_{2,0}$ are different, while those on $g^a_{1,0}$ and $g^b_{2,0}$ are the same. Note that the partial wave amplitude expansion of $g^a_{1,0}+g^b_{2,0}$ is not symmetric under the transformation $\rho^{1111}_\ell\leftrightarrow\rho^{2222}_\ell$. Thus, we can predict that the extrema of the $g^a_{1,0}+g^b_{2,0}$ bounds are achieved when $\rho^{1111}_\ell\neq\rho^{2222}_\ell$, leading to different bounds using the linear and nonlinear unitarity conditions. The $g^b_{2,0}$ case is just the opposite. As for $g^a_{1,0}$, its extrema can be achieved by setting $\rho^{1122}_\ell=0$, in which case (A16) is automatically satisfied due to (A15). Thus, for $g^a_{1,0}$, the linear and nonlinear unitarity conditions are the same, which leads to the same positivity bounds.

DOI: 10.52396/JUSTC-2023-0159
JUSTC, **2024**, 54(7): 0705